3 RESULTS

3.1 Analysis of a balanced translocation t(2;10)(q31.1;q26.3) in a male patient with SPD

Disease-associated balanced chromosomal rearrangements (DBCR) form a unique resource in linking genotypes and phenotypes. Therefore mapping of chromosomal breakpoints in patients with DBCR is a very powerful approach to identify disease genes (Bugge et al. 2000). Moreover, the same method can be a good starting point to investigate regulatory elements controlling gene expression (Fantes et al. 1995; Lauderdale et al. 2000; Kleinjan et al. 2001; Griffin et al. 2002). In order to obtain more data about molecular mechanisms leading to limb development in humans, a detailed cytogenetic and molecular study on a balanced translocation t(2;10)(q31.1;q26.3) in a male patient with limb defects was performed.

3.1.1 Clinical description of the male patient with a de novo balanced translocation t(2;10)(q31.1;q26.3)

The patient is a thirteen-year-old boy carrying an apparently balanced chromosome rearrangement t(2;10)(q31.1;q26.3) (schematically depicted in Fig. 5*A*). He is the second child of healthy unrelated parents, born after normal pregnancy without fetal distress. Clinical examination after birth revealed severe malformations of hands and feet as well as a dysmorphic face. The hands were short, had 6 fingers, and absence of the distal phalanges including the nails was noted. The feet showed complete absence of toes II to V and a rudimentary first toe with a missing distal phalanx. X-rays of the hands showed 5 short metacarpals and 6 digits, each consisting only of a single phalanx (Fig. 5*B*-*C*). Metacarpal III was bifurcated at its end giving rise to two digits. The patient was not able to fully extend his elbows and knees due to contractions. Bilateral inguinal hernias were noted and surgically corrected. X-rays of the thorax showed hypoplasia of the medial ends of both clavicles. Ultrasound of the skull revealed hypoplasia of the cerebellum. Further clinical examinations demonstrated developmental delay, deep set eyes (left > right) a progressive scoliosis, narrow shoulders, ataxia, coxa valga, and short stature (110 cm at age 6, < p3). The patient received

several surgical corrections of the hands including removal of polydactylous digits. He has developed well and is currently attending a special school.

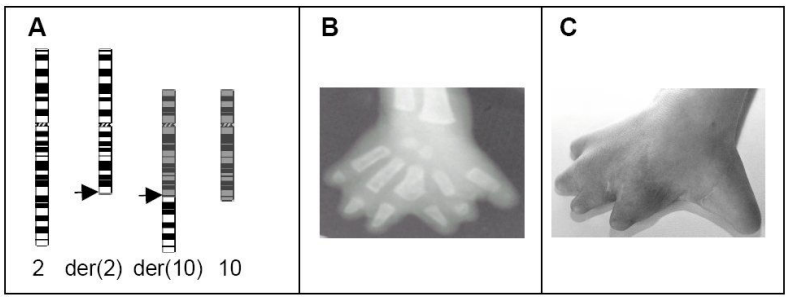

Fig. 5 *A*: Schematic representation of chromosomes in the patient with the translocation t(2;10)(q31.1;q26.3). Breakpoints at 2q31.1 and 10q26.3 are marked with arrows. *B,C*: An X-ray and a photo of the right hand of the patient after surgical correction.

3.1.2 Cytogenetic investigation of the chromosomal breakpoints in the patient

Breakpoint mapping was performed using the fluorescence *in situ* hybridisation (FISH) technique. Several large genomic clones were selected from the regions of interest and were hybridised to the patient's metaphase chromosomes. Number and localisation of detected signals helped to narrow down the breakpoint regions (see Fig. 6*A*).

For the chromosome 2 breakpoint, YAC clone 751E12 (with marker D2S2257 located at 188 cM) gave signals on chromosome 2 and der(2), which indicates that this clone lies proximal to the breakpoint. Another YAC clone, 785G8 (with markers D2S148 and D2S2173 located at 190 cM) showed signals on chromosome 2 and der(10), thus being distal to the breakpoint (data not shown). Thereby, the breakpoint region on chromosome 2 was narrowed down to a 2 cM long interval. This region contains several genes, among others the *HOXD* genes, which were considered as interesting candidates for the patient's phenotype. In order to investigate, whether the translocation disrupts the *HOXD* cluster, BAC clone RP11-514D19 (GenBank acc. no. AC016915), containing the *EVX2* and *HOXD8-13* genes, were hybridised to the patient's chromosomes. The results indicated that this clone lies distal to the breakpoint (Fig. 6*B*). Additional hybridisation experiments with a series of BAC clones selected from the region proximal to *EVX2* led to the identification of the breakpoint-spanning clone RP11-538A12 (GenBank acc. no. AC016761) (Fig. 6*C*).

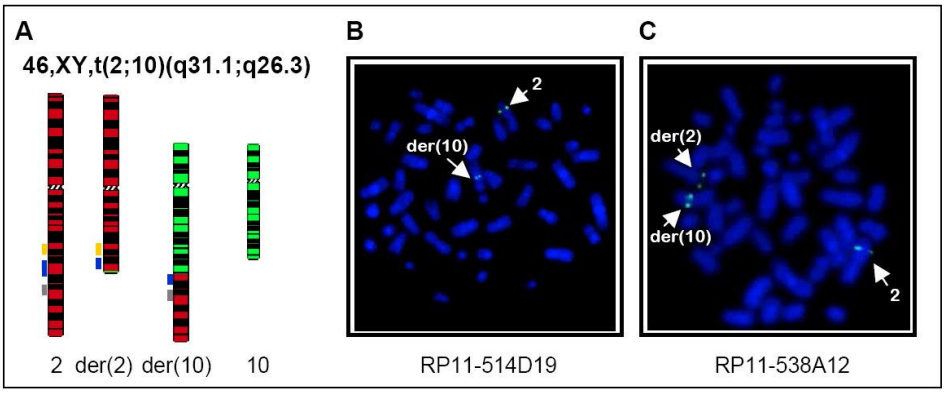

Fig. 6 *A*: Principle of FISH. Genomic clones from the breakpoint region on chromosome 2 (yellow, blue and red bars) are used as hybridisation probes on patient metaphase chromosomes. The breakpoint-spanning clone (blue) shows signals on the normal chromosome 2, the derivative 2 [der(2)] and the derivative 10 [der(10)]. For a proximal (yellow) or a distal (red) clone, only two signals are detected in each case: on chromosome 2 and der(2) or chromosome 2 and der(10), respectively. *B*: FISH results showing hybridisation of BAC clone RP11-514D19 to patient's chromosomes. Signals on chromosomes 2 and der(10) indicate that the clone lies distal to the breakpoint. *C*: FISH results showing hybridisation of the breakpoint-spanning clone RP11-538A12 to patient's chromosomes; signals were detected on chromosome 2, der(2) and der(10) (indicated by arrows).

To map the breakpoint more precisely, PCR products generated with primers selected from the clone RP11-538A12 were used for screening the chromosome 2-specific cosmid library. Positive clones were hybridised to the patient chromosomes, and as a result the proximal and distal cosmids, LLNLc128A0237 and LLNLc128F0946 respectively, were identified. Sequencing of the cosmid ends, together with database searches, revealed that these clones slightly overlap by approximately 0.9 kb. The overlapping sequence lies in an approximately 4.5 kb long LINE repeat, thus the region covering this repeat and extending at least 3 kb in both directions was considered as the region of interest, where the breakpoint must have occurred.

Breakpoint mapping on chromosome 10 was performed in a similar way. YAC 743G11, one of six clones that have been tested, gave signals on der(10), which placed the breakpoint distal to the marker D10S1201. Further mapping showed that BAC RP11-300B2 (GenBank acc. no. AL355531) was breakpoint spanning (not shown). Moreover, BACs RP11-267K7 (GenBank acc. no. AL359508) and RP11-290N15 (GenBank acc. no. AC022688) were found to be proximal and clones 218C11 (GenBank acc. no. AL353725) and 355P15 (GenBank acc. no. AC011849) to be distal to the breakpoint (Fig. 7 and data not shown). BLAST searches

combined with information from the UCSC Genome Browser Gateway database allowed establishing a contig, which indicated the overlapping regions between the proximal and the breakpoint-spanning BACs, as well as between the breakpoint-spanning clone and the distal ones. The common regions have been excluded from further investigation, and an approximately 60 kb region found solely on the breakpoint-spanning BAC has been considered as the candidate region (see Fig. 7).

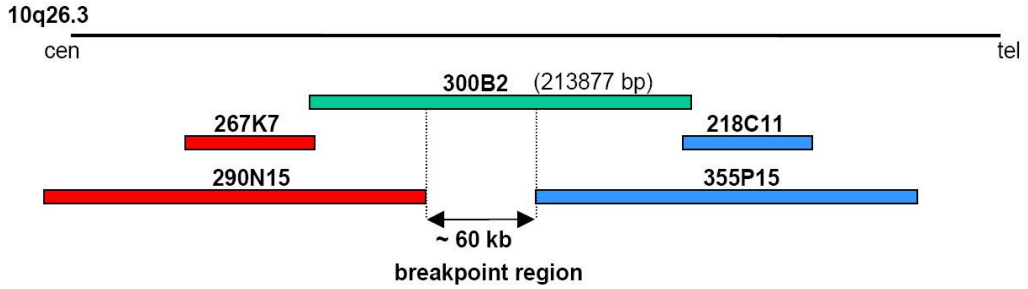

Fig. 7 BAC contig on chromosome 10q26.3. The breakpoint-spanning BAC 300B2 is shown in green, proximal BACs are shown in red and distal BACs in blue. The breakpoint region is located between the distal and the proximal BACs.

3.1.3 Southern blot experiments and cloning of the breakpoints

In order to localise precisely the breakpoint on chromosome 2, patient and control DNAs were digested with several restriction enzymes and transferred onto nylon membranes. Probes derived from the candidate region were radioactively labelled and hybridised to the blots. The probe 538A12_49750 gave aberrant restriction fragments in patient DNA digested with *Bam*HI or *Hin*dIII, whereas the more centromeric probe 538A12_79400 showed aberrant restriction fragments in patient DNA cut with *Bgl*II or *Pst*I. Analysis of the restriction site positions narrowed down the breakpoint region to approximately 1 kb (Fig. 8*A*).

Mapping of the chromosome 10 breakpoint was performed in a similar way, although the candidate region was much larger. Initially, eight probes from the 60 kb long breakpoint region were amplified and hybridised to digested patient and control DNAs. Two probes, 300B2_80000 and 300B2_90000 gave additional bands seen in patient DNA cleaved with *Hpa*I and not in the control. Moreover, different lengths of the aberrant restriction fragments observed with these two probes indicated that the breakpoint maps between these probes, thus is located between 80778 bp and 90997 bp on the breakpoint-spanning BAC (data not

shown). In order to refine the breakpoint region, several new probes were designed and used for hybridisation. As a result, aberrant bands were obtained with probe 300B2_84000 in the *Mbo*I or *Ssp*I digest. This allowed narrowing down the breakpoint region to approximately 700 bp (Fig. 8*B*).

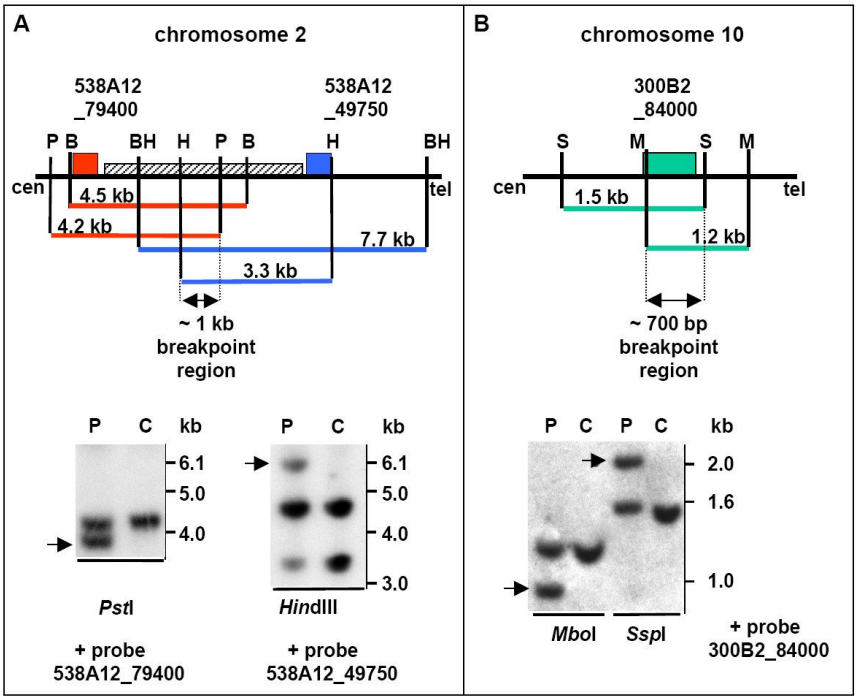

Fig. 8 *A*: Schematic representation of the breakpoint region on BAC RP11-538A12 and the localisation of probes 538A12_79400 and 538A12_49750 (shown as red and blue boxes, respectively) used for Southern blot hybridisation. Positions and sizes of normal restriction fragments are indicated and enzymes are marked as follows: B = *Bgl*II, BH = *Bam*HI, H = *Hin*dIII, P = *Pst*I. The striped box between the two probes indicates the LINE repeat. Lower panels: Southern blot analysis with probes 538A12_49750 and 538A12_79400. DNAs from the patient (P) and a control (C) were digested with *Pst*I or *Hin*dIII restriction enzymes. Aberrant bands present only in the patient and not in the control (arrows), indicate that the breakpoint on chromosome 2 is located within the *Pst*I and *Hin*dIII restriction fragments (approximately 1 kb long). Probe 538A12_49750 recognises in addition to the normal 3.3 kb long *Hin*dIII restriction fragment also another fragment of approximately 4.6 kb in both patient and control DNAs.

B: Schematic representation of the breakpoint region on BAC RP11-300B2. Probe 300B2_84000 is shown as the green box. Positions and sizes of normal restriction fragments are indicated and enzymes are marked as follows: S = *Ssp*I, M = *Mbo*I. Lower panel: Southern blot hybridisation of the probe 300B2_84000 to patient (P) and control (C) DNAs digested with *Ssp*I or *Mbo*I restriction nucleases. Additional bands (shown with arrows) present only in patient and not in control DNAs indicate that the breakpoint on chromosome 10 is located within the *Ssp*I and *Mbo*I restriction fragments (approximately 700 bp long as shown in the upper panel).

In order to clone the breakpoints on both chromosomes, adaptors were ligated to the patient DNA digested with *Eco*RI enzyme. Subsequent PCR reactions with adaptor and sequence specific primers gave rise to two products, approximately 500 bp long for the der(10) and approximately 1.1 kb long for the der(2), which were subcloned and sequenced. The results indicated that the breakpoint on chromosome 2 is located between positions 107910 bp and 107912 bp of clone RP11-538A12. The nucleotide G at position 107911 bp is missing, moreover on der(2) a 9 bp long insertion is present between the original chromosome 2 and chromosome 10 sequences. The breakpoint on chromosome 10 occured between positions 85078 bp and 85079 bp of BAC RP11-300B2 (Fig. 9).

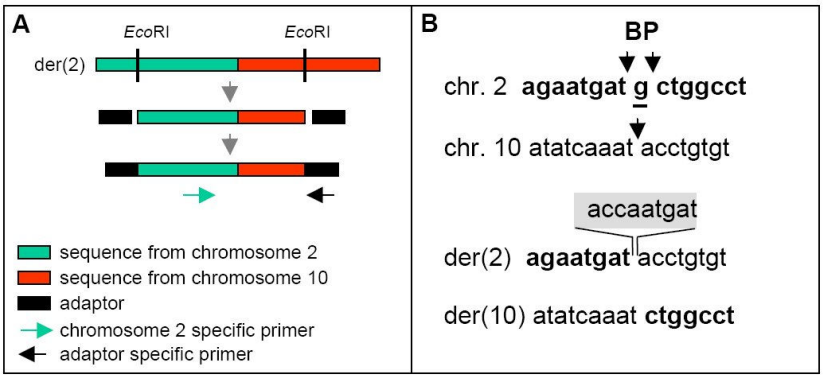

Fig. 9 *A*: Principle of breakpoint cloning. For simplicity only one derivative chromosome [der(2)] is shown. Genomic DNA from the patient was digested with *Eco*RI restriction enzyme. The restriction fragments were then ligated to adaptors on both ends. The junction fragments were amplified by PCR using primers specific for the sequence on chromosome 2 and for the sequence of the adaptor. Sequencing of the PCR products showed the exact sites of the chromosome 2 and chromosome 10 breakpoints.

B: Chromosome 2, 10, der(2) and der(10) sequences in the translocation patient. Chromosome 2-derived sequences are shown in bold, the underlined guanine residue from chromosome 2 is missing in both derivative chromosomes. The 9-bp insertion of unknown origin within der(2) (shaded box) separates chromosome 2- and chromosome 10-derived sequences.

3.1.4 The *MGMT* gene is disrupted by the breakpoint but it is still expressed from the intact chromosome 10 in the translocation patient

Computational analysis of the breakpoint region on chromosome 10 indicated that the breakpoint-spanning BAC 300B2 contains the methylguanine-DNA methyltransferase gene (*MGMT*) encoding a DNA-repair enzyme. The breakpoint occurred between exons 1 and 2 of

MGMT, upstream of the ATG codon (Fig. 10). Therefore one allele of this gene must be inactive in the patient.

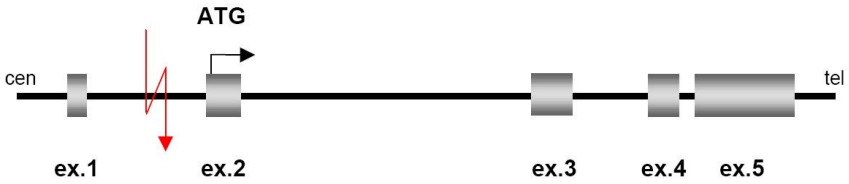

Fig. 10 Organisation of the *MGMT* gene. Five exons span over 300 kb of genomic DNA (not drawn to scale). The breakpoint in the translocation patient (marked in red) disrupted *MGMT* between exons 1 and 2.

In order to examine the expression of *MGMT* in the patient, RT-PCR and Northern blot experiments have been performed. Both approaches indicated that the expression of *MGMT* is maintained in the patient lymphoblastoid cell line. Moreover, Northern blot results suggested that the amount of the *MGMT* mRNA compared to the total mRNA (represented by the housekeeping gene *G3PDH*) is lower in the patient than in control cell lines (Fig. 11*A*). Quantification analysis performed using the ImageQuant software confirmed that the intensity of the *MGMT* signals in the patient is approximately two times lower than in controls. This result is in agreement with the previous data which indicated that in the patient one of the *MGMT* alleles has been disrupted by the breakpoint.

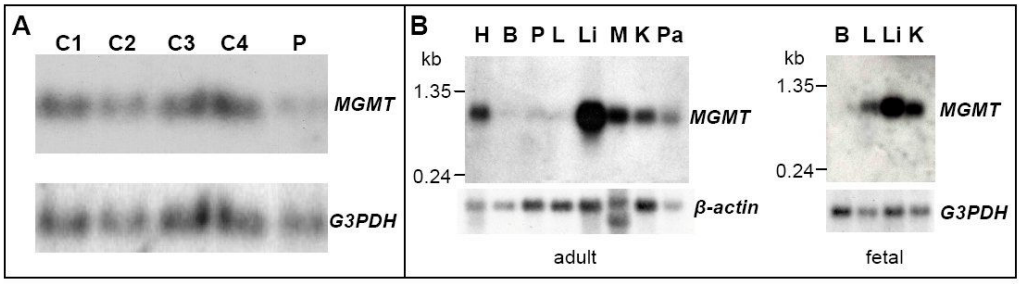

Fig. 11 *A*: Northern blot hybridisation of the *MGMT* probe (exons 2-4) to four different control (C1, C2, C3 and C4) and patient (P) total RNAs. *G3PDH* served as a control for RNA loading. The *MGMT* signal is lower in the patient compared to the controls. *B*: Hybridisation of the same *MGMT* probe to human multiple tissue Northern (MTN) blots shows ubiquitous expression in adult and foetal tissues. H = heart, B = brain, P = placenta, L = lung, Li = liver, M = skeletal muscle, K = kidney, Pa = pancreas. The length of the detected transcript corresponds to the literature data (Nakatsu et al. 1993). *β-actin* or *G3PDH* served as a control for RNA loading.

Moreover, the *MGMT* probe was hybridised to commercial human multiple tissue Northern blots from adult and foetal tissues. The results showed ubiquitous expression of this gene in different tissues, with the highest level of expression in liver and the lowest in brain (Fig. 11*B*).

3.1.5 Analysis of the breakpoint region on chromosome 2

3.1.5.1 The breakpoint on chromosome 2 does not disrupt any known gene

Sequencing of the breakpoint region revealed the exact position of the chromosome 2 break, which appeared to lie approximately 390 kb away from the *HOXD* genes (see Fig. 12). To clearify whether there is any gene disrupted on chromosome 2 or not, the region around the breakpoint has been analysed.

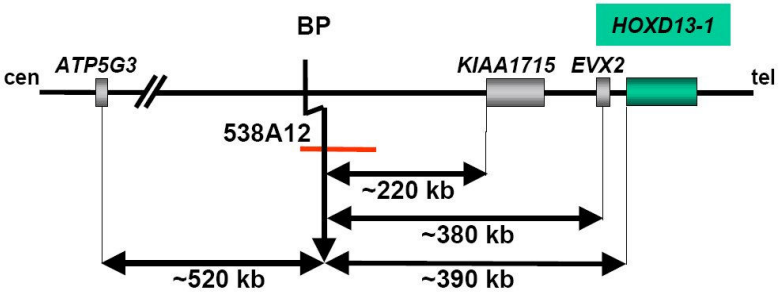

Fig. 12 Schematic map of the breakpoint region on chromosome 2q31.1. The breakpoint spanning BAC clone RP11-538A12 is shown in red. Known genes neighbouring the breakpoint (BP) are schematically depicted (boxes). The *HOXD* cluster containing 9 genes is represented by the green box. Approximate distances between genes are indicated (not drawn to scale). Cen and tel indicates the orientation of the centromere and the telomere, respectively.

First, the NIX program was used to find known genes and ESTs. The complete sequence of the breakpoint-spanning BAC 538A12 was analysed but there were no obvious genes found on this clone. However, there were good matches to 14 EST sequences derived from colon, breast, uterus or testis. All ESTs were collinear with the genomic sequence and corresponded to nine different positions in the genome. Since it was not clear whether the ESTs were parts of genes or just genomic contaminations, RT-PCR experiments were performed. All primers were first tested on human genomic DNA and only working primer pairs were used for

further experiments. Lack of appropriate human tissues was the reason for using human cell lines as the RNA source for RT-PCR. None of the ESTs could be amplified using 35 PCR cycles, but few of them gave products after 70 cycles. However, such a high number of cycles required for amplification of the putative ESTs suggests that they are probably genomic contaminations rather than expressed sequences. Therefore, it is very likely that there are no genes located on the breakpoint-spanning clone.

The list of putative ESTs and the RT-PCR results can be found in appendix (section 11.5).

3.1.5.2 The HOXD13 gene is not mutated in the patient

HOXD genes located on chromosome 2 were shown to cause limb abnormalities in humans and in mice. Especially, different mutations in the *HOXD13* gene cause synpolydactyly (SPD) (Goodman et al. 1997; Goodman et al. 1998; Calabrese et al. 2000; Debeer et al. 2002; Kan et al. 2003). Since SPD can be observed in the patient described in this study, it was theoretically possible that his phenotype is caused by a mutation in *HOXD13*, rather than by the translocation. In order to test this hypothesis, the whole coding sequence and parts of the intron of *HOXD13* in the patient were amplified (see Fig. 13) and sequenced. The results did not show any mutation within the entire *HOXD13* gene, hence the patient's phenotype is most probably caused by the translocation.

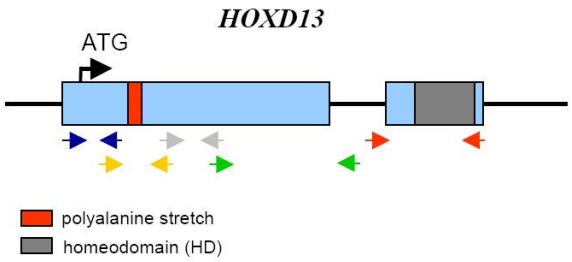

Fig. 13 Schematic representation of the human *HOXD13* gene. Two exons (blue) encode the nuclear homeoprotein. Regions coding for conserved domains are marked with red and grey. For *HOXD13* amplification, five different primer pairs (coloured arrows) were used. Not drawn to scale.

3.1.5.3 The human sequence upstream to the breakpoint shows high homology to the corresponding region in mouse

Abnormal limb development in the patient with a translocation t(2;10)(q31.1;q26.3) suggests involvement of *HOXD* genes in the origin of the phenotype. However, *HOXD13* in the proband is neither mutated nor directly truncated by the translocation. These data gave rise to

the hypothesis that the translocation might have changed expression of *HOXD* genes by disturbing their normal regulation. This in turn might have resulted in the limb phenotype of the patient. I focused my interest on the region centromeric to the breakpoint, since this part of chromosome 2 was separated from the *HOXD* cluster in the translocation patient (see also Fig. 12), and might contain important regulatory elements necessary for proper *HOXD* expression.

In theory, highly conserved non-coding sequences are good candidates for regulatory elements, thus sequence comparison between different species is generally considered to be useful in the identification of gene enhancers or silencers. Since this approach has already been successfully implemented (Loots et al. 2000), I decided to use it in my study. Approximately 130 kb of human sequence lying centromeric to the breakpoint were compared to the corresponding mouse region (approximately 70 kb long) using the PipMaker programme. As a result, 45 elements equal or longer than 100 bp and showing at least 70% identity between human and mouse were found. Five of these elements are associated with human EST sequences BG952464, AW937867 and BE064736, and their expression (except for EST BE064736) was confirmed by RT-PCR in human cell lines or in brain (data not shown). One sequence corresponds to the mouse EST AK015352 expressed in testis. It was not clear whether the other 39 elements are coding or not. In order to test this, RT-PCR experiments with primers specific for these elements were performed on RNA from mouse stage E16.5. Because of the high similarity between human and mouse genes, it was justified to use mouse instead of human RNA for RT-PCR analysis. Moreover, mouse tissues were much more easily accessible. All tested sequences but one could not be amplified using less than 70 PCR cycles, suggesting that they might be non-coding. In conclusion, with this approach it was not possible to reduce significantly the number of putative regulatory elements and to create a good basis for further tests. For this reason functional analyses of the candidate regions have not been pursued.

The list of putative candidates for regulatory sequences with their characteristics is presented in appendix (section 11.6).

3.2 Screening for Hoxd13 interaction partners

As the sequencing of the human genome is completed, the focus of research is shifting to the functional analysis of gene products. Most proteins do not act alone, instead they interact with each other or with other components of a cell. Thus, a very complex structural and functional network is formed. Therefore, one of the very important tasks in molecular biology is not only to study the function of an isolated protein, but also to identify its interacting partners. This knowledge provides new clues about the normal function of the protein in the cell. Moreover, this knowledge is indispensable in understanding the molecular events leading to proper or abnormal development of our body. Since my interest was focused on molecular bases of limb development, in the second part of my project I have searched for Hoxd13 interaction partners.

3.2.1 Yeast two-hybrid screen as a commonly used method to identify protein-protein interactions

One of the most commonly used methods allowing identification of protein-protein interactions is the yeast two-hybrid system. This technique takes advantage of the fact that transcription factors require two functional domains in order to activate gene expression. One of these domains is responsible for DNA binding (BD - **b**inding **d**omain), whereas the second one, called activation domain (AD), induces transcription. In the yeast two-hybrid system these two domains are physically separated and therefore they cannot activate genes, however bringing both of them into close proximity allows reconstitution of a fully active transcription factor.

In this study, the mouse Hoxd13 protein (bait) has been fused to the DNA-binding domain derived from the prokaryotic LexA protein. Proteins from a mouse embryonic library (preys) were fused to the activation domain originating from the viral protein VP16. The bait and prey fusion proteins were expressed in L40 yeast strain, which contains LacZ and HIS3 marker genes under the control of the LexA operon. Induction of the reporter genes could occur only when a prey protein from the library interacts with Hoxd13, resulting in spatial association of the LexA DNA binding domain and the VP16 activation domain (Fig. 14). Expression of HIS3 is normally assayed by growth on media lacking histidine and *LacZ*

expression can be monitored by colorimetry or other methods detecting β-galactosidase activity.

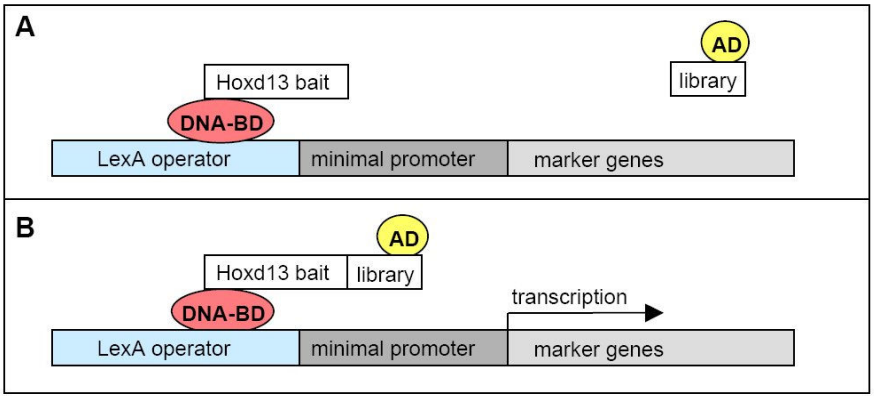

Fig. 14 Yeast two-hybrid principle. *A*: Hoxd13 fused to the LexA DNA-binding domain (DNA-BD) can bind the LexA operator but is not able to activate transcription of the marker genes (*HIS3* and *LacZ*) by itself. Library proteins fused to the activation domain (AD) cannot bind DNA and therefore marker genes are not expressed. *B*: Interaction between Hoxd13 and a specific library protein brings both the DNA binding and activation domains together which allows transcription of the *HIS3* and *LacZ* marker genes (adapted from Matchmaker LexA Two-Hybrid System, User Manual, BD Biosciences).

3.2.2 Construction of the bait vector

The yeast two-hybrid method is based on creation of a novel transcriptional activator. Therefore, in order to obtain reasonable results using this technique, it is essential to use a bait lacking transcriptional activity. This prerequisite seems to exclude transcription factors as possible baits, especially if it is not clear which domain of the protein possesses transcriptional activity. However, the structure of Hoxd13 is known quite well. Similarly to its human homologue (for the gene structure see: Fig. 13), mouse Hoxd13 contains a polyalanine (poly-Ala) repeat in the N-terminal region and a homeodomain (HD) located at the C-terminus. It has been proposed that the N-terminus is responsible for protein-protein interactions (Shen et al. 1996), whereas the homeodomain is known to bind DNA and activate transcription. Therefore, to generate the construct without transcriptional activity, it was necessary to use Hoxd13 lacking the homeodomain.

Construction of the bait vector for the yeast two-hybrid screen included RT-PCR amplification and cloning of the N-terminal part of mouse *Hoxd13* (*Hoxd13-HD*) into the pBMT116 vector containing the bacterial LexA DNA-binding domain and carrying the *Trp1*

marker gene (the pBMT116 map can be found in appendix, section 11.2). The resulting construct, called LexA_Hoxd13-HD (Fig. 15*A*), should generate a fusion protein consisting of the LexA DNA-binding domain at the N terminus followed by the mouse Hoxd13 sequence without homeodomain.

Before the yeast two-hybrid analysis was carried out, expression of this protein had been confirmed in yeast. Shortly, cell lysates were prepared from yeast transformed with the LexA_Hoxd13-HD construct and from the non-transformed control, and loaded on a polyacrylamide gel. Western blot analysis using anti-LexA specific antibodies allowed detection of a band of approximately 50 kDa, corresponding to the expected size of the LexA_Hoxd13-HD fusion protein, only in the transformed cells (Fig. 15*B*).

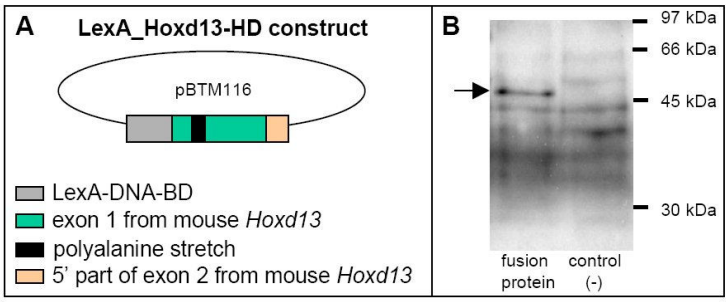

Fig. 15 *A*: Schematic representation of the bait construct used for the yeast two-hybrid screen. Exon 1 and the 5' end of exon 2 from the mouse *Hoxd13* gene have been cloned into the pBTM116 vector, downstream to the LexA DNA-binding-domain-encoding gene (LexA-DNA-BD). The part of *Hoxd13* coding for the homeodomain (3' end of exon 2) has not been included in the bait vector. *B*: Western blot showing expression of the LexA_Hoxd13-HD fusion protein in yeast. Anti-LexA antibodies detect a band of approximately 50 kDa only in cells transformed with the LexA_Hoxd13-HD construct (arrow), whereas no band of this size can be detected in the non-transformed control.

Furthermore, potential auto-activation activity of the LexA_Hoxd13-HD construct has been examined. As the first step, yeast cells carrying the LexA_Hoxd13-HD vector were streaked on SD plates lacking tryptophane and histidine (SD –TH). Single colonies which appeared after 4-5 days on SD –TH plates suggested that the bait alone could be able to activate the *HIS3* marker gene (not shown). However, it is also known that the *HIS3* promoter in the L40 yeast strain possesses basal activity even in the absence of bait-prey interactions. To overcome this problem, 3-amino-1,2,4-triazole (3-AT) which is a competitive inhibitor of the

HIS3 gene product, is usually added to the yeast medium. Testing of several different concentrations of 3-AT indicated that upon addition of 10 mM 3-AT no yeast colonies could grow on SD -TH plates (data not shown). Thus, under these conditions the LexA_Hoxd13-HD fusion protein was not capable to activate expression of the marker gene, hence it was suitable for the yeast two-hybrid screen.

3.2.3 Yeast two-hybrid screen

To co-express bait and prey proteins, yeast cells carrying the LexA_Hoxd13-HD bait construct were transformed with the mouse embryonic cDNA library cloned in the pVP16 vector. For a negative control, the bait was co-transformed with the empty pVP16 vector. After transformation, yeast cells were plated in parallel on SD plates lacking tryptophane and leucine (SD –TL) to check for transformation efficiency, and on SD plates lacking tryptophane, histidine, uracil, leucine and lysine (SD –THULL) supplemented with 10 mM 3-AT to detect interactions.

Colonies on the SD –TL plates were observed already 2 days after transformation and their number indicated that approximately 1.6×10^8 clones were screened. This means that the library, which has approximately 5×10^6 clones, was covered more than 30 times in the screen. The first positive colonies on the SD –THULL plates were seen 3 days after transformation, and they have been collected every 24 hours starting at day 4 and finishing at day 7 after transformation. At the same time, no colony growth was observed on the control plate, indicating that there was no unspecific interaction between the bait and the prey vector (Fig. 16).

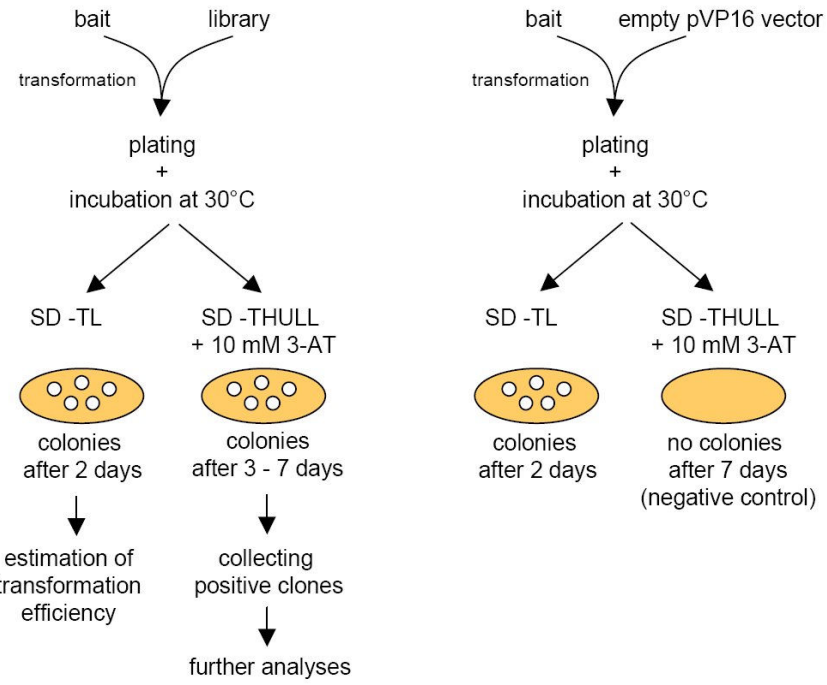

Fig. 16 Scheme of the yeast two-hybrid screen. Bait and prey constructs were co-expressed in yeast cells. After incubation at 30°C on selective plates (SD -THULL), positive yeast colonies were collected and the isolated prey clones were further analysed. For the negative control, the bait was co-transformed with the empty prey vector into yeast cells. Lack of colonies on SD -THULL medium indicated that the bait itself cannot activate marker genes. Colony growth on SD -TL medium served as a positive control of transformation.

However, due to technical limitations, a yeast two–hybrid screen usually generates a large number of false-positive interactions. In order to facilitate the identification of true positives, different approaches were implemented. First, collected clones were re-streaked 3 times on fresh SD –THULL plates. Afterwards, the expression of the second marker gene (*LacZ*) was examined in all HIS3-positive clones. In a colony-lift filter assay only 138 clones showed a strong blue staining, and these double positives ($HIS3^+/LacZ^+$) were used for further analysis. The rest of the clones showed either much weaker or no detectable expression of β-galactosidase (see Fig. 17). A summary showing the number of positive colonies picked after the screen is shown in Table 25.

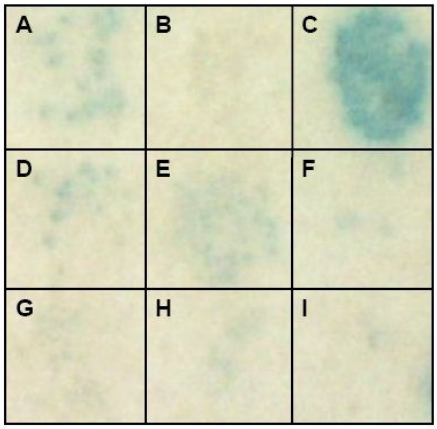

Fig. 17 Colony-lift filter assay. HIS3-positive clones were transferred to Whatman paper filters. The enzymatic reaction was performed using X-Gal as substrate. Blue staining indicates that the *LacZ* marker gene coding for β-galactosidase is expressed in yeast. Results are shown only for eight HIS3-positive clones (panels A and C-I; each panel corresponds to a single yeast clone). Panel B represents the negative control (yeast clone transformed with the LexA_Hoxd13-HD construct and the empty pVP16 vector). Only the clone seen in panel C showed intensive blue staining and therefore it was considered as a potential Hoxd13 interaction partner.

Table 25 Results of the screen showing the number of positive colonies

Day after transformation	No. of $HIS3^+$ colonies collected	No. of $HIS3^+$ colonies with intensive blue staining
4	128	22
5	252	38
6	182	26
7	401	52
Total	963	138

3.2.4 Analysis of positive colonies

Double positive clones ($HIS3^+$/$LacZ^+$) collected after the screen were re-streaked on fresh SD –THULL plates, and used for colony PCR in order to amplify the prey inserts. PCR products were sequenced with pVP16-specific primers and obtained sequences were subjected to BLAST against public databases at NCBI. The results of this analysis revealed that the positive preys represent 53 different genes. Among them, 2 hits were within 3' UTRs, whereas 51 hits matched to ORFs. Out of these 51 ORF-specific hits, 37 genes were cloned in frame, 3 were not in frame and 11 were cloned in the antisense orientation. The list of 37 genes represented by preys cloned in frame can be found in Table 26.

Table 26 List of genes found in the yeast two-hybrid screen

Gene name	GenBank accession no.	Process/function
Dlxin-1	AB029448	Limb development
Peg10	AB091827	Chromatin / RNA binding
Cnot3	NM_146176	
Dazap2	NM_011873	
Pax3	NM_008781	
Tead2	NM_011565	
Snrp70	AK077425	
Snrp116	NM_011431	
Pold4	AF515709	Proliferation / apoptosis
Nedd9	NM_017464	
Bat3	NM_057171	
Pins	AY081187	
Limk1	NM_010717	Protein modification / signal transduction
Ppp2ca	NM_019411	
Ddr2	NM_022563	
Map4k4	NM_008696	
Pkm2	NM_011099	Cellular metabolism and movement
Bckdha	NM_007533	
Pla2g4b	BC016255	
Mical3	NM_153396	
Kifc5a	NM_053173	
Itch	AF037454	
Ubce7ip3	AF124663	
Angptl2	NM_011923	Secreted / extracellular matrix proteins
Fbln2	NM_007992	
Fn1	NM_010233	
Col18a1	NM_009929	
mKIAA1046	AK122429	Unknown function
mKIAA0863	AB093268	
mKIAA0054	AB093209	
mKIAA0222	NM_183033	
Drpla	NM_007881	
Bcap37	NM_007531	
Odz3	NM_011857	
Rnf38	NM_175201	
Wtip	NM_207212	
Limd1	NM_013860	

3.2.5 Peg10 as a putative Hoxd13 interaction partner

Among the candidate genes found in the yeast two-hybrid screen *Peg10* was represented by 8 different clones. *Peg10* (GenBank accession no. AB091827) is transcribed into an approximately 6.4 kb long transcript with two long open reading frames (ORFs). ORF1 encodes a putative zinc finger domain of the CCHC class commonly found in the Gag protein of retroviruses. ORF2 has the potential to encode a polypeptide containing a consensus motif for an aspartyl protease catalytic site, which is characteristic for retroviral proteases. Similarly as in retroviruses, these two ORFs overlap and the ribosomal frameshift can lead to production of a long polyprotein (Fig. 18) (Shigemoto et al. 2001; Manktelow et al. 2005).

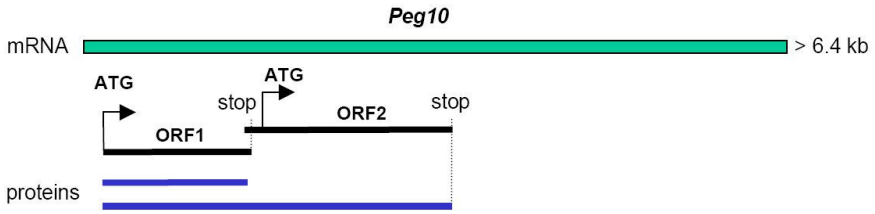

Fig. 18 *Peg10* and ribosomal slippage mechanism. *Peg10* mRNA encodes two open reading frames, ORF1 and ORF2. Translation of the transcript gives rise to two proteins. The first protein corresponds to ORF1, whereas the second one to both ORF1 and ORF2. The longer protein is generated by ribosomal slippage which leads to a frameshift and abolishment of the first stop codon. The next recognised termination codon is present at the end of ORF2.

All *Peg10* clones found in the yeast two-hybrid screen correspond to ORF2 and are cloned in frame. Their localisation within the gene can be seen in Fig. 19. Since some clones contain overlapping sequences, only five of them were used for further analysis.

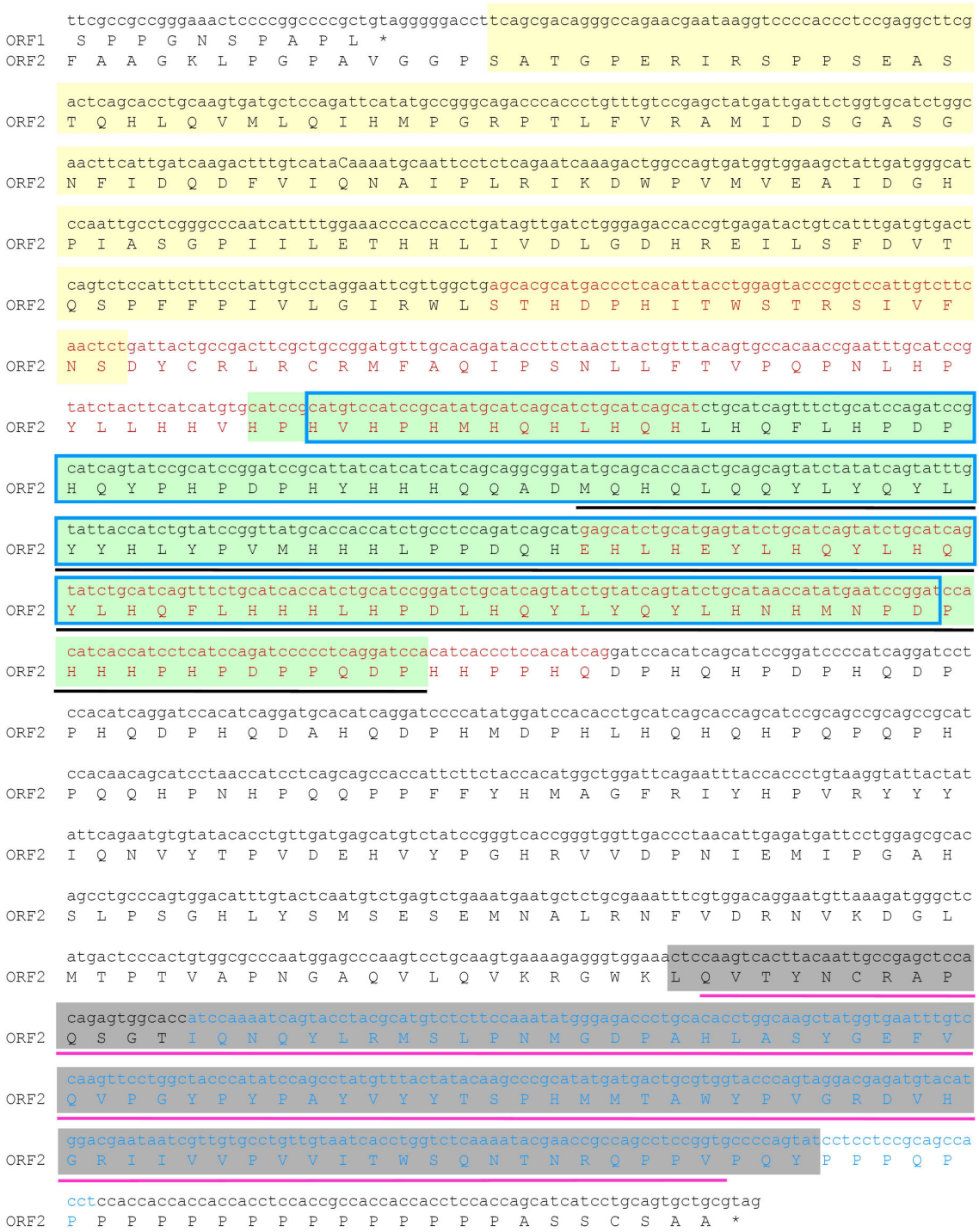

Fig. 19 Part of the *Peg10* gene sequence corresponding to the end of ORF1 and the complete ORF2 (according to the GenBank entry AB091827). Clones found in the yeast two-hybrid screen are marked as follows: clone no. 649 - light yellow box; clone no. 318 - red letters; clone no. 40 - light green box; clone no. 81 - blue frame; clone no. 37 - black underline; clone no. 22 - blue letters; clone no. 173 - grey box; clone no. 143 - pink underline.

3.2.5.1 Confirmation of the interaction with Hoxd13-HD in LexA and GAL4 systems

Prey plasmids corresponding to the *Peg10* gene were isolated from five positive clones numbered 37, 40, 143, 318 and 649 (Fig. 19 shows their inserts sequences). To confirm the interaction between preys and Hoxd13-HD in yeast, wild type L40 cells were co-transformed separately with the bait (LexA_Hoxd13-HD construct) and every single prey plasmid. Moreover, preys were co-transformed with the empty pBTM116 vector (bait vector) in order to test them for autoactivation. Growth on SD –THULL medium observed only for colonies transformed with the bait and a prey indicates interaction between Hoxd13-HD and parts of Peg10 fragments in the LexA system (Fig. 20).

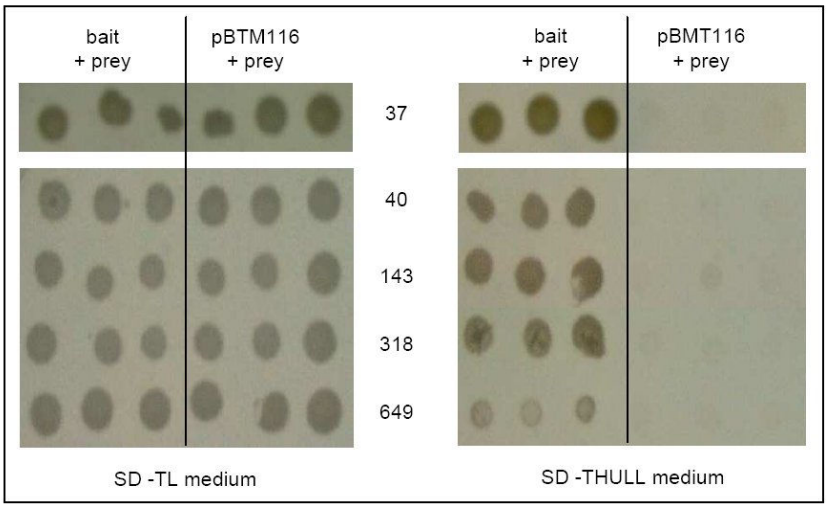

Fig. 20 Yeast cells co-transformed with the LexA_Hoxd13-HD bait or pBTM116 empty vector and one of the *Peg10* prey plasmids (numbers 37, 40, 143, 318 or 649) were spotted in triplicates on selective media. Colony growth on SD -TL plates indicates that both plasmids entered the cell (positive control of transformation), whereas presence of colonies on SD –THULL medium confirms the interaction between Hoxd13 lacking the homeodomain and different Peg10 fragments. Specificity of these interactions is proven by absence of colonies which carry a prey and the empty bait plasmid (pBTM116) on SD -THULL medium.

In addition, the cDNA for Hoxd13 lacking the homeodomain (Hoxd13-HD) was cloned into the pGBKT7 bait vector containing the GAL4 DNA-binding domain. Sequencing of the construct and expression analysis of the fusion protein performed by Western blot indicated that the GAL_Hoxd13-HD bait could be used in yeast two-hybrid experiments. Similarly as for the LexA_Hoxd13-HD construct, the GAL_Hoxd13-HD bait was co-transformed with the isolated prey plasmids. Expression of nutrition marker genes visualised by the growth of

yeast colonies on selective media indicated that the interactions between different parts of Peg10 and the Hoxd13 protein take also place in the GAL4 yeast system (data not shown).

3.2.5.2 Cloning of Peg10

Since the yeast two-hybrid method usually generates a lot of false positives, any interaction discovered in yeast has to be confirmed in the mammalian system as well. The prerequisite for this includes cloning the gene of interest into a mammalian expression vector. There are two identical GenBank entries representing the full length *Peg10* gene (AB091827 and NM_130877), moreover their alignment with the *Edr* gene (GenBank ID: AJ006464) suggests that all three sequences correspond to the same gene (sequence alignment can be found in appendix, section 11.7). Two significant differences between AB091827 and AJ006464 are present in the 5' region of both sequences (resulting in various N-termini of the predicted open reading frames) and in the length of the repeat which lies within ORF2.

As all *Peg10* clones found in the yeast two-hybrid screen corresponded to ORF2, my interest was focused on this particular part of the gene. To determine its real sequence, ORF2 was amplified in eight independent RT-PCR reactions performed on mouse cDNAs derived from four different embryonic stages. All RT-PCR products appeared to be identical, suggesting that the true sequence of the *Peg10* ORF2 was obtained. However, comparison of the RT-PCR product with the GenBank entries AB091827 and AJ006464 showed that all three sequences differ in the length of imperfect repeats present in the gene (Fig. 21). Interestingly, the various lengths of the QDPH-encoding repeats do not cause frameshifts, therefore all putative proteins have the same C-terminus.

Repetitive sequences are usually difficult to clone, since they are prone to various rearrangements during bacterial replication. However, special *E.coli* strains increasing insert stability have been designed. One of them, the recombinase-deficient STBL4 *E.coli* strain, was used for cloning *Peg10* ORF2 into the mammalian expression vector pcDNA-Flag. In spite of much effort (isolation and analysis of 35 transformants), cloning of the full length RT-PCR product corresponding to the ORF2 was not successful. All analysed clones carried mutations, mostly deletions, within the repetitive region of *Peg10*. In three analysed plasmids, the inserts appeared to be identical to the *Peg10* sequence represented by the GenBank entry AB091827. One of these clones, named Peg10-ORF2_pcDNA-Flag was used for further experiments.

```
AJ006464-ORF2  AATCCGGATCCACATCACCACTCTCATCCAGATCCCCCTCAGGATCCACATCACCCTCCA
RT-PCR_product AATCCGGATCCACATCACCATCCTCATCCAGATCCCCCTCAGGATCCACATCACCCTCCA
AB091827-ORF2  AATCCGGATCCACATCACCATCCTCATCCAGATCCCCCTCAGGATCCACATCACCCTCCA

AJ006464-ORF2  CATCAGGATCCACATCAGCATCCGGATCCCCATCAGGAT--------------------
RT-PCR_product CATCAGGATCCACATCAGCATCCGGATCCCCATCAGGATCCTCCACATCAGGATCCACAT
AB091827-ORF2  CATCAGGATCCACATCAGCATCCGGATCCCCATCAGGAT--------------------

AJ006464-ORF2  ------------------------------------------------------------
RT-PCR_product CAGCATCCGGATCCCCATCAGGATCCTCCACATCAGGATCCACATCAGCATCCGGATCCC
AB091827-ORF2  ------------------------------------------------------------

AJ006464-ORF2  ------------------------------------------------------------
RT-PCR_product CATCAGGATCCTCCACATCAGGATCCACATCAGGATGCACATCAGCATCAGGATCCCCAT
AB091827-ORF2  ------------------------------------------------------------

AJ006464-ORF2  ------GCACATCAGGATCCCCATCAGGATCCCCATCAGGATGCACATCAGGATCCACAT
RT-PCR_product CAGGATGCACATCAGGATCCCCATCAGGATCCCCATCAGGATGCACATCAGGATCCACAT
AB091827-ORF2  ------------------------------------------------------------

AJ006464-ORF2  CAGCATCCGGATCCCCATCAGGATCCTCCACATCAGGATCCACATCAGGATGCACATCAG
RT-PCR_product CAGCATCCGGATCCCCATCAGGATCCTCCACATCAGGATCCACATCAGGATGCACATCAG
AB091827-ORF2  ------------------------CCTCCACATCAGGATCCACATCAGGATGCACATCAG
```

Fig. 21 Sequence comparison between the RT-PCR product and GenBank entries AB091827 and AJ006464 corresponding to the ORF2 of *Peg10*. For simplicity, only the region containing imperfect repeats is shown. Differences in the nucleotide sequences are marked in red.

3.2.5.3 Immunocytochemistry studies

For cellular localisation studies, the Peg10-ORF2_pcDNA-Flag construct was transfected into COS1 cells and the protein was detected with anti-Flag specific antibodies. The results indicated that the protein is present in the cytosol (Fig. 22).

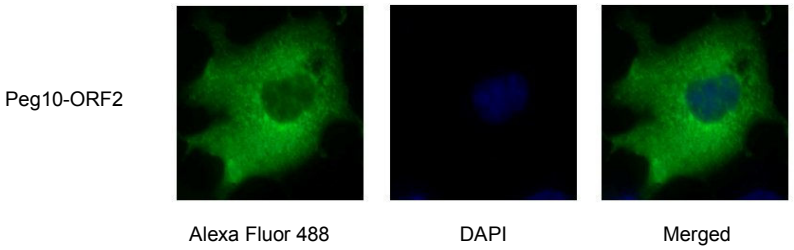

Fig. 22 Cytosolic localisation of Peg10-ORF2 (green) in transiently transfected COS1 cells. The nucleus is visualised by the DAPI-staining (blue).

A similar experiment was performed with different Hoxd13 expression constructs, namely wtHoxd13-pTL1-HA2 (carrying the full length Hoxd13), Hoxd13-HD-pTL1-HA2 (containing Hoxd13 lacking the homeodomain), Hoxd13+14Ala-pTL1-HA2 (containing Hoxd13 with the Ala stretch expanded for fourteen additional alanine residues) and Hoxd13_2Ala-pTL1-HA2 (carrying Hoxd13 with the Ala stretch reduced to two alanines). The results showed that wild type and Hoxd13_2Ala proteins localise to the nucleus, whereas the mutant lacking the homeodomain as well as the Hoxd13+14Ala are present in the cytosol, building aggregate-like structures (Fig. 23). All observed signals were specific, since the transfection of COS1 cells with empty pcDNA-Flag or pTL1-HA2 vectors resulted in no fluorescently labelled cells (data not shown).

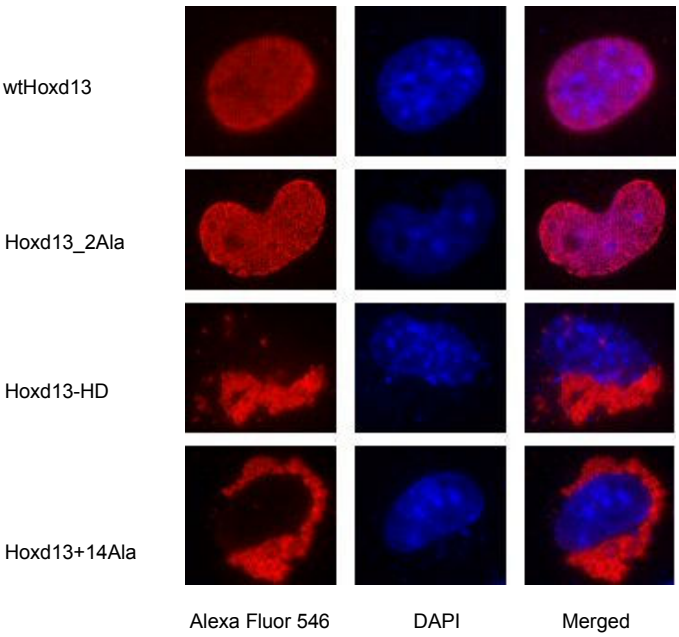

Fig. 23 Single transfection of COS1 cells with the constructs carrying wild type or mutant *Hoxd13*. Red signals indicate cellular localisation of wild type and mutant Hox proteins. Nuclei are labelled with DAPI (blue).

In the next step, different Hoxd13 constructs were co-expressed with Peg10-ORF2 in COS1 cells, in order to examine the putative interaction between the proteins. In all double-transfected cells, Peg10-ORF2 perfectly co-localised with cytosolic aggregates formed by Hoxd13-HD or Hoxd13+14Ala proteins (Fig. 24). Moreover, although Peg10 is detected only in the cytosol of single transfected COS1 cells, it can be seen in the nucleus of COS1 cells co-expressing either the full length Hoxd13 or Hoxd13_2Ala (Fig. 24). However, co-localisation in the nucleus was seen only in approximately 20% of double-transfected cells.

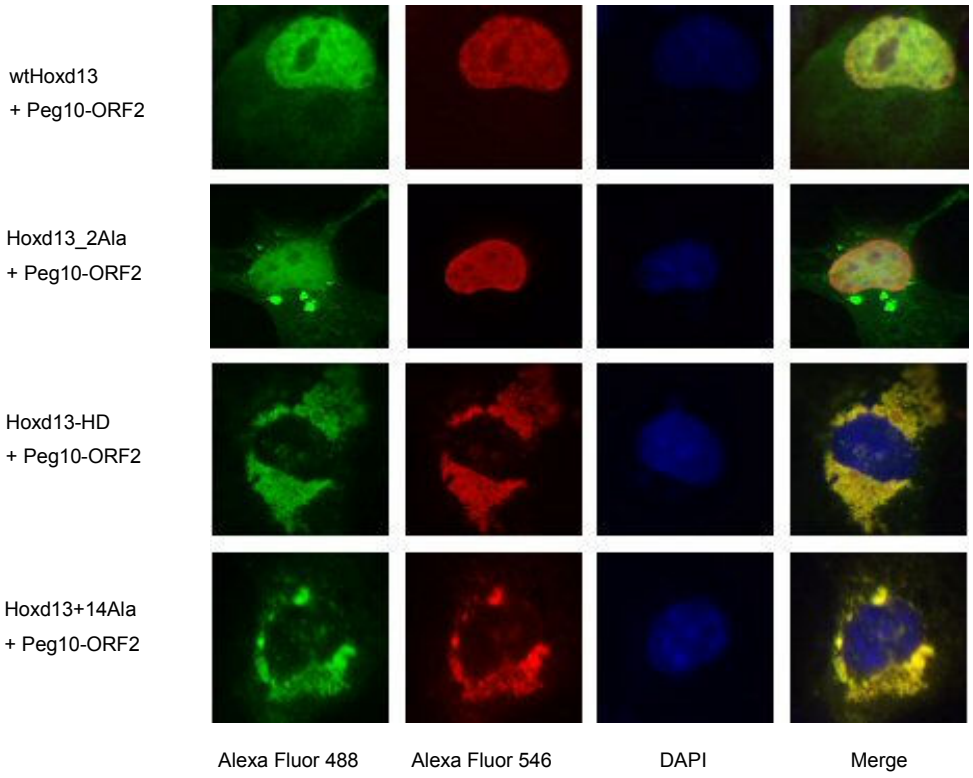

Fig. 24 Co-localisation of Peg10-ORF2 (green) with wild type and mutant Hoxd13 proteins (red) in COS1 cells. Peg10-ORF2 expression can be observed in the nucleus (stained with DAPI in blue) of cells co-transfected with wtHoxd13 or Hoxd13_2Ala. Cells co-transfected with the Peg10-ORF2_pcDNA and Hoxd13-HD-pTL1-HA2 or Hoxd13+14Ala-pTL1-HA2 constructs show co-localisation of both proteins in the cytosol.

3.2.5.4 Coimmunoprecipitation assay

The co-localisation results suggested that the Hoxd13 protein could interact with Peg10. In order to confirm this, coimmunoprecipitation studies have been performed. In preliminary experiments, COS1 cells were transfected separately with different HA-tagged Hoxd13 constructs or with Peg10-ORF2_pcDNA-Flag. Western blot analysis of the cell lysates indicated that all proteins were easily detectable with polyclonal anti-HA or anti-Flag antibodies, respectively (data not shown).

The immunoprecipitation was performed with anti-Flag antibodies, followed by detection of the Hoxd13 proteins with anti-HA antibodies. The results indicated that all Hoxd13 proteins could bind Peg10-ORF2 (Fig. 25*A*). Later, these results were confirmed by additional

experiments, in which the immunoprecipitation with anti-HA antibodies was followed by Peg10 detection with anti-Flag antibodies (Fig. 25*B*).

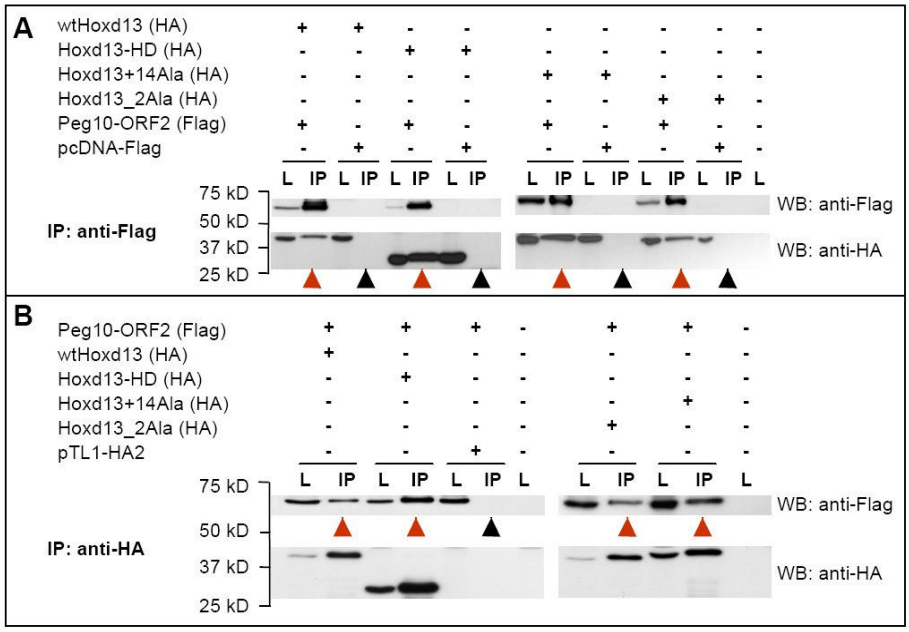

Fig. 25 Coimmunoprecipitation results. *A*: COS1 cells were co-transfected with different HA-tagged Hoxd13 constructs and with the Flag-tagged Peg10-ORF2 or the empty pcDNA-Flag vector (for negative controls). Cell lysates were used for precipitation with anti-Flag beads. In each case, lysates (L) and precipitates (IP) were run on polyacrylamide gels, followed by protein detection with anti-tag antibodies. Precipitation efficiency can be seen on anti-Flag blots (positive controls), whereas protein-protein interactions are detected using anti-HA antibodies. Hoxd13 proteins co-precipitate with Peg10-ORF2 (red arrowheads) but they cannot be pulled down by the empty pcDNA-Flag vector (black arrowheads), indicating specificity of interaction. *B*: Confirmation of Hox-Peg10 binding after antibody switch. Hoxd13 proteins were precipitated with anti-HA beads, shown on anti-HA blots. Peg10-ORF2 was pulled down together with Hox proteins (red arrowhead) but not with the empty pTL1-HA2 vector (black arrowheads), as shown on anti-Flag blots.

3.2.5.5 Whole-mount and section in situ hybridisation

The results obtained in the immunocytochemistry and coimmunoprecipitation assays strongly suggest that Hoxd13 wild type and mutant proteins could bind Peg10. However, these experiments were performed in an artificial system and it is not clear, whether these two proteins could interact *in vivo*. In order to address this question, whole mount *in situ* hybridisation was performed. An antisense probe for the *Peg10* gene was hybridised to mouse embryos from stages E10.5, E11.5 and E12.5. The results indicated that at the earlier stages

(E10.5) *Peg10* is present in most distal parts of the limb buds, however this domain seems to expand more posteriorly in E11.5 old limb buds. At a later stage (E12.5) *Peg10* is expressed in digits and the proximal limb region (Fig. 26). Section *in situ* hybridisation performed on E13.5 and E15.5 limbs showed *Peg10* signals in digits, metacarpals, carpals and in limb muscles. This pattern differs from *Hoxd13* expression domains (Fig. 27).

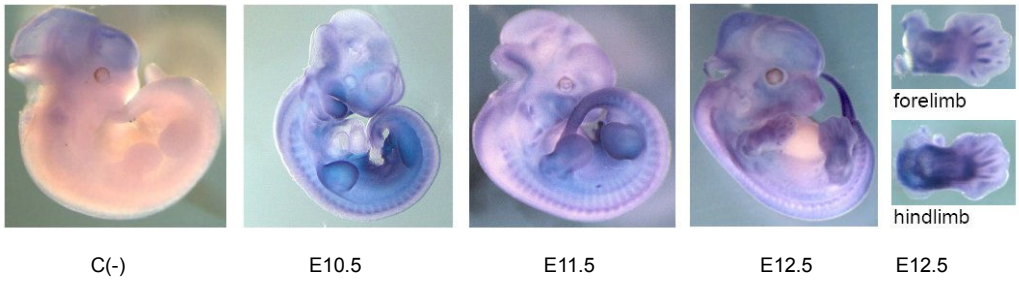

Fig. 26 Whole mount *in situ* hybridisation showing expression of *Peg10* during mouse embryonic development. *Peg10* is clearly upregulated in limb buds and in the tail tip (blue signals). Negative control [C(-)] shows no staining in both structures, indicating that the *Peg10* signal is specific. For the E12.5 stage, in addition to the whole embryo, magnified images of a fore- and a hindlimb are shown.

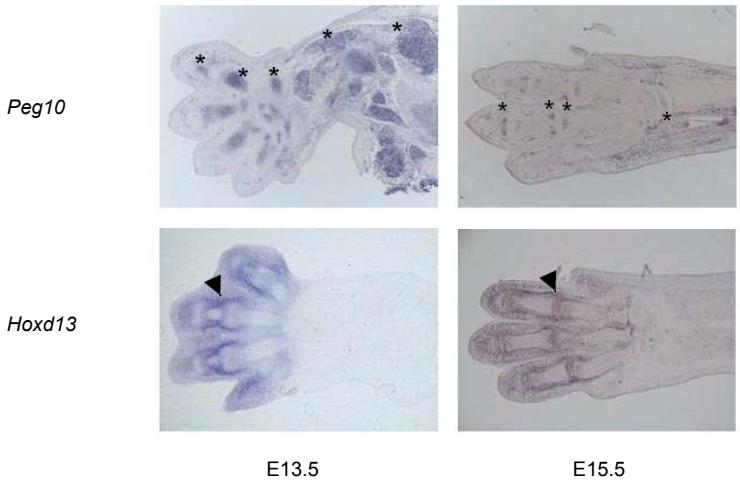

Fig. 27 Section *in situ* hybridisation showing expression of *Peg10* and *Hoxd13* in mouse limbs. At stage E13.5, *Peg10* transcripts are present in the condensations of phalanges, metacarpals and carpals, as well as in muscles (asterisks). *Hoxd13* shows a different expression pattern, being present in the perichondrium (arrowhead). At stage E15.5, both genes seem to maintain their expression pattern, however *Peg10* signals in the distal limb are very weak. Hybridisation of gene-specific probes was performed on paraffin sections (stage E13.5) or cryo-sections (E15.5).

3.2.6 Investigation of other putative Hoxd13 binding proteins

In addition to *Peg10*, five other genes identified in the yeast two-hybrid screen were considered as promising candidate Hoxd13 binding partners. Co-expression of each single clone with LexA_Hoxd13-HD or with GAL_Hoxd13-HD in yeast, confirmed interactions between the candidates and Hoxd13 in both LexA and GAL4 two-hybrid systems (not shown). Further experiments including cellular localisation studies in COS1 cells as well as *in situ* hybridisation are presented in the following sub-sections.

3.2.6.1 Studies on Dlxin-1

The first interesting gene, for which two slightly different clones have been found in the yeast two-hybrid screen, is called *Dlxin-1* or *Maged1* (**m**elanoma **a**nti**ge**n, family **D**, **1**) and it shows a limb-specific expression pattern (Matsuda et al. 2003). The longer prey plasmid isolated in the screen contains a 349 bp long insert (1252–1600 bp according to the GenBank entry AB029448) which covers the region encoding the WQXPXX repeat of the Dlxin-1 protein. This domain is known to interact with Dlx5, a homeobox-containing transcription factor important for limb development (Masuda et al. 2001). The same WQXPXX repeat together with the second distinctive domain of Dlxin-1, the necdin homology domain (NHD), have been shown to be necessary for binding of Msx2, another homeodomain-containing transcription factor which plays a role in osteoblast differentiation. The NHD alone binds Ror2, a receptor tyrosine kinase, mutations of which are causative for limb pathologies: brachydactyly type B (OMIM #113000) or Robinow syndrome (OMIM #268310) (Matsuda et al. 2003). All these data made Dlxin-1 an interesting candidate for a Hoxd13-interaction partner.

Transfection of COS1 cells with pcDNA-Flag vector carrying the 349 bp long *Dlxin-1* fragment isolated in the yeast two-hybrid screen, and subsequent immunocytochemistry studies revealed that the truncated Dlxin-1 protein localises to the cytosol (Fig. 28). Co-transfection with the wtHoxd13-pTL1-HA2 construct did not influence the cellular localisation of the truncated Dlxin-1 protein (Fig. 28), suggesting that Hoxd13 and Dlxin-1 do not bind each other in COS1 cells.

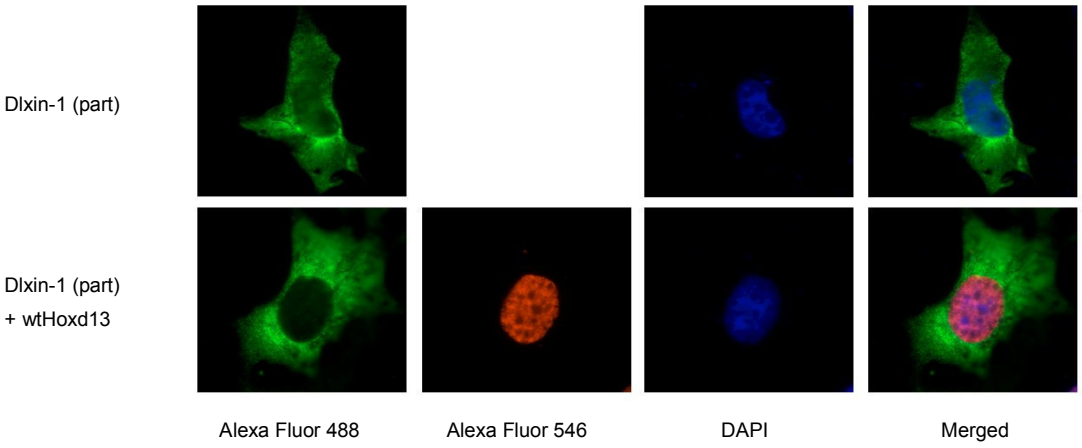

Fig. 28 Overexpression of the Dlxin-1 construct in COS1 cells. Truncated Dlxin-1 (green) localises to the cytosol and does not change its cellular localisation in cells co-transfected with wild type Hoxd13 (red). Cell nuclei are stained with DAPI in blue.

3.2.6.2 LIM domain-containing genes

Among putative Hoxd13 binding partners, three LIM domain-containing proteins were identified in the yeast two-hybrid screen, Wtip (GenBank accession number NP_997095), Limk1 (GenBank accession number NP_034847) and Limd1 (GenBank accession number NP_038888). LIM domains are cysteine- and histidine-rich domains which bind two zinc ions. They appear to mediate protein-protein interactions and are found in many key regulators of developmental pathways (Dawid et al. 1998).

Wtip gene (WT1-interacting protein also known as similar to LIM domains containing 1) has been represented by a single prey clone with the insert covering the region encoding two LIM domains. Whole mount *in situ* hybridisation of the *Wtip* probe to mouse embryos (E10.5 and E11.5) showed a limb specific expression pattern of this gene. Moreover, it has been shown that the Wtip protein binds Ror2, the receptor tyrosine kinase indispensable for normal skeletal development (Verhey van Wijk, not published). Overexpression of full length Wtip in COS1 cells indicated that the protein is localised in the cytosol (Fig. 29) and does not co-localise with Hoxd13 in nuclei of cells co-transfected with the wtHoxd13-pTL1-HA2 construct (Fig. 29).

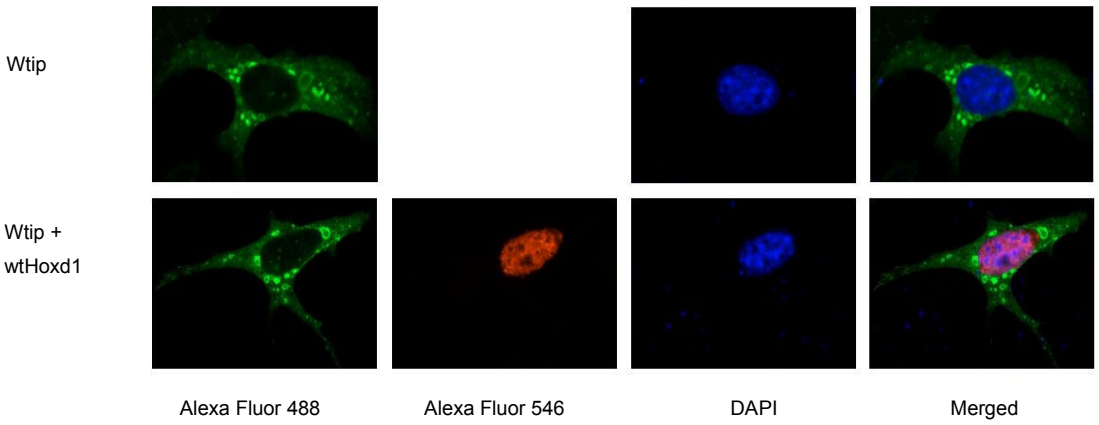

Fig. 29 Overexpression of Wtip in COS1 cells. Wtip (green) localises to the cytosol in single-transfected cells. Co-transfection with the wtHoxd13_pTL1-HA2 construct (red signal) does not influence Wtip cellular localisation. Blue staining (DAPI) marks cell nuclei.

Limk1 (LIM-domain containing protein kinase) is the second LIM protein identified as a potential Hoxd13 interaction partner. The protein contains two LIM domains, a PDZ- and a kinase domain, and it has not been connected to limb development yet. Interestingly, it has been shown that the human homologue, LIMK1, can shuttle between the cytosol and the nucleus (Yang and Mizuno 1999) and is involved in Golgi dynamics, membrane traffic and cytoskeletal organisation (Stanyon and Bernard 1999; Rosso et al. 2004). Two prey clones encoding the Limk1 protein were identified in the yeast two-hybrid screen, the shorter one covers 380-830 bp and the longer one 317-794 bp within the *Limk1* sequence NM_010717. The LIM domain-encoding region is included in both inserts. The shorter *Limk1* fragment was subcloned into the mammalian expression vector pcDNA-Flag and used for cellular localisation studies. The results indicated that the partial Limk1 protein shows both cytosolic and nuclear localisation when overexpressed in COS1 cells, suggesting a possible interaction with the wild type Hoxd13 in the nucleus. However, the same truncated Limk1 protein does not seem to co-localise with the aggregates formed by Hoxd13 lacking the homeodomain (Fig. 30). Whole mount *in situ* hybridisation performed with the *Limk1*-specific probe showed ubiquitous expression of this gene in mouse embryos (E10.5 – E12.5) (Fig. 31).

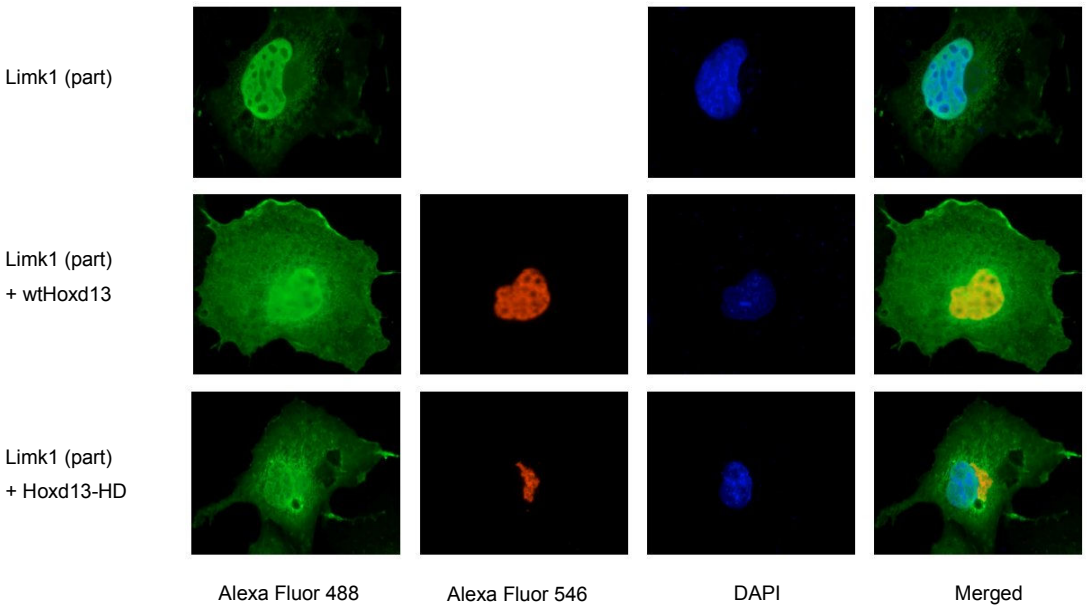

Fig. 30 Partial Limk1 protein (green) is present in both the cytosol and the nucleus (blue) of single-transfected COS1 cells. Upon co-transfection with the wild type Hoxd13 or Hoxd13-HD (red signals) there is no detectable change in the localisation of the partial Limk1 protein.

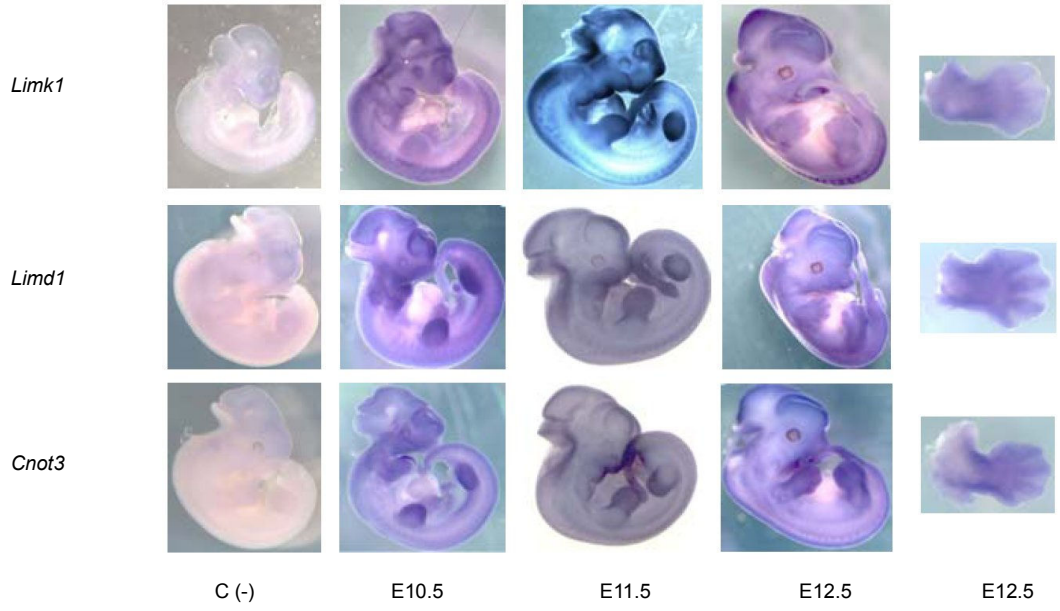

Fig. 31 Whole mount *in situ* hybridisation showing expression of *Limk1*, *Limd1* and *Cnot3* (blue) during mouse embryonic development. All three genes are expressed in limb buds, however *Limk1* expression seems to be more ubiquitous. Negative controls [C(-)] show only very slight staining in the head, indicating specificity of detected signals. For stage E12.5, in addition to the whole embryo, magnified images of forelimbs are shown.

Limd1 (LIM domains containing 1) is a novel gene, being very poorly characterised so far. The human LIMD1 protein is a tumor suppressor. Its ability to bind the retinoblastoma protein (pRB), allows shuttling of LIMD1 between the cytosol and the nucleus (Sharp et al. 2004). Sequence analysis of mouse Limd1 revealed that the protein contains three LIM domains, which according to the yeast two-hybrid data, might be responsible for Hoxd13 binding. In order to examine the expression pattern of *Limd1* during mouse embryonic development, whole mount *in situ* hybridisation experiments were performed. The results showed that *Limd1* is expressed in mice limb buds (Fig. 31). For further analysis, the *Limd1* fragment identified in the yeast two-hybrid screen (1974–2287 bp within the GenBank entry NM_013860), was cloned into the pcDNA vector and overexpressed in COS1 cells. Single transfection experiments indicated that the partial Limd1 protein is present throughout the whole cell. Co-expression with the wild type Hoxd13 or with Hoxd13-HD showed co-localisation of the partial Limd1 protein with both Hoxd13 proteins (Fig. 32).

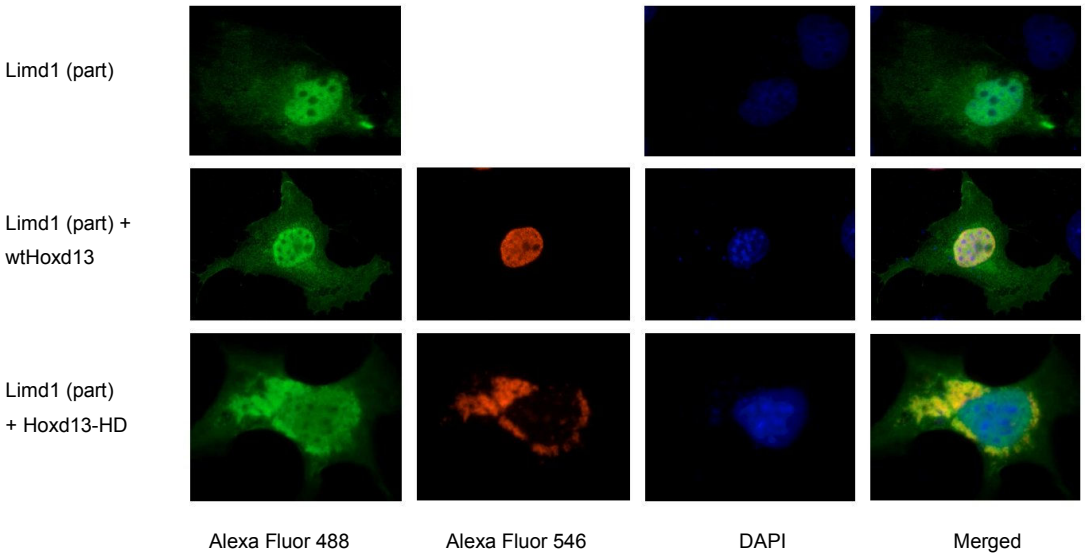

Fig. 32 Overexpression of the truncated Limd1 protein in COS1 cells. Single transfection shows that Limd1 (green) is localised in the nucleus (labelled with DAPI in blue) and spreads in the whole cytosol. Double transfections with wtHoxd13 proteins (red) show co-localisation of both proteins in the nucleus. Furthermore, co-expression with Hoxd13 lacking the homeodomain (red), changes Limd1 pattern in the cytosol, suggesting a possible interaction between both proteins.

3.2.6.3 Cnot3 as a putative Hoxd13 binding partner

Cnot3 (GenBank accesion number NM_146176) encodes a subunit of the CCR4-NOT complex which is known to control global gene expression. Furthermore, it has been shown that mouse and human Cnot3 orthologues can bind other transcriptional regulators (Aoki et al. 2002; Yin et al. 2005). Cnot3 protein has a proline-serine rich region at the C-terminus and two coiled-coil domains at the N-terminus; the function of the latter ones is not clear. The only prey clone corresponding to *Cnot3* which was found in the yeast two-hybrid screen, covers the region encoding the second coiled-coil domain (639–941 bp within the GenBank entry NM_146176).

In order to perform cellular localisation studies, the short prey insert was overexpressed in COS1 cells, either alone or together with *Hoxd13* constructs. The results indicated that the partial Cnot3 protein co-localises with both the wild type Hoxd13 protein and its N-terminal part (Fig. 33). Whole mount *in situ* hybridisation showed that *Cnot3* is expressed in embryonic limb buds (Fig. 31) and therefore it is possible that it could interact with Hoxd13 in order to regulate expression of target genes.

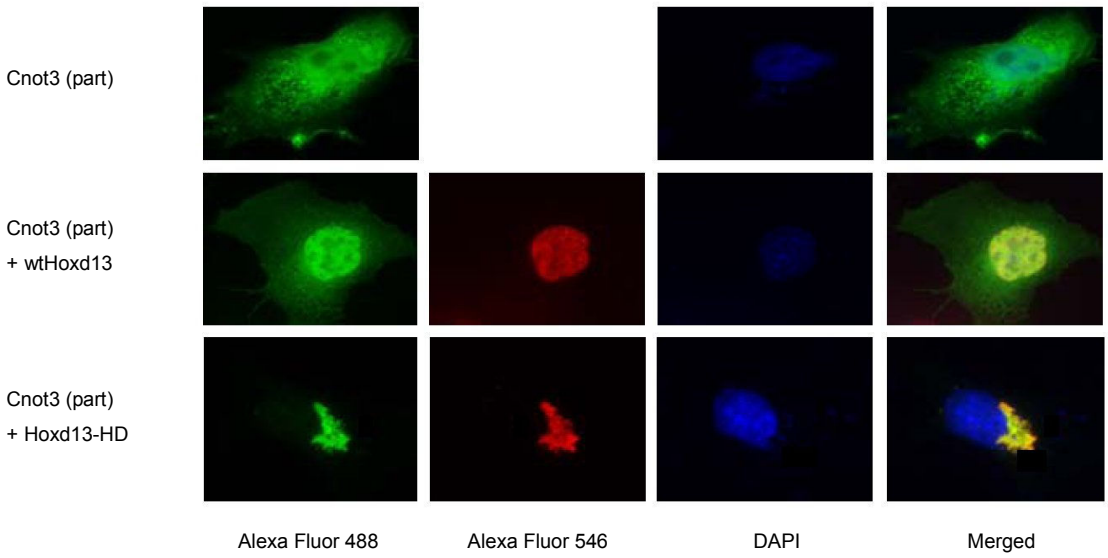

Fig. 33 Overexpression of the partial Cnot3 protein in COS1 cells. Single transfection shows that Cnot3 (green) is localised in the cytosol and the nucleus (labelled with DAPI in blue). Double transfections with Hoxd13 proteins (red signals) indicate that the Cnot3 fragment co-localises in the nucleus with the wild type Hoxd13 and in the cytosol with Hoxd13 lacking the homeodomain.